MASLEN, E. N., STRELTSOV, V. A. & STRELTSOVA, N. R. (1993*a*). *Acta Cryst.* **B49**, 636–641.
MASLEN, E. N., STRELTSOV, V. A. & STRELTSOVA, N. R. (1993*b*). *Acta Cryst.* **B49**, 980–984.
NAGEL, S. (1985). *J. Phys. C*, **18**, 3673–3685.
PRINCE, E. (1982). *Mathematical Techniques in Crystallography and Materials Science*. New York: Springer-Verlag.
REES, B. (1977). *Isr. J. Chem.* **16**, 180–186.
SALASCO, L., DOVESI, R., ORLANDO, R., CAUSA', M. & SAUNDERS, V. R. (1991). *Mol. Phys.* **72**, 267–277.
SATOW, Y. (1992). Private communication.
SATOW, Y. & IITAKA, Y. (1989). *Rev. Sci. Instrum.* **60**, 2390–2393.
STEVENS, E. D. (1974). *Acta Cryst.* A**30**, 184–189.
STRELTSOV, V. A. & MASLEN, E. N. (1992). *Acta Cryst.* A**48**, 651–653.
TSIRELSON, V. G., ANTIPIN, M. YU., GERR, R. G., OZEROV, R. P. & STRUCHKOV, YU. T. (1985). *Phys. Status Solidi A*, **87**, 425–433.
ZACHARIASEN, W. H. (1967). *Acta Cryst.* A**23**, 558–564.

Acta Cryst. (1993). B**49**, 980–984

X-ray Study of the Electron Density in Magnesite, $MgCO_3$

BY E. N. MASLEN, V. A. STRELTSOV AND N. R. STRELTSOVA

Crystallography Centre, University of Western Australia, Nedlands 6009, *Australia*

(*Received* 25 *December* 1992; *accepted* 28 *June* 1993)

Abstract

The electron density in a naturally faced mineral crystal of $MgCO_3$ was re-measured with Mo $K\alpha$ (λ = 0.71073 Å) diffraction data, using extinction corrections that minimize differences between equivalent reflection intensities. The deformation electron density has 0.66 e Å^{-3} density maxima in the C—O bonds and 0.35 e Å^{-3} maxima at the O-atom lone pairs. Space group $R\bar{3}c$, hexagonal, M_r = 84.31, a = 4.635 (1), c = 15.023 (2) Å, V = 279.5 (1) Å^3, Z = 6, D_x = 3.005 Mg m^{-3}, μ(Mo $K\alpha$) = 0.48 mm^{-1}, $F(000)$ = 252, T = 293 K, R = 0.022, wR = 0.025, S = 5.87 for 332 unique reflections.

Introduction

Carbonate minerals derive their identity from the CO_3 group which typifies coherent, non-molecular structure segments that act as rigid bodies. Analysis of the CO_3 group's rigid-body vibrations in magnesite (Finger, 1975) shows translation and libration motions parallel to and about the c axis, and in the plane normal to c. Disorder of that CO_3 group, consistent with a rigid-body riding motion was suggested by early authors, but no positional disorder in the planar CO_3 anion was observed in deformation electron-density ($\Delta\rho$) maps by Göttlicher & Vegas (1988), who explained the maps in terms of ionic interactions between Mg and CO_3 ions. The $\Delta\rho$ topography at the middle of the Ca—O vector in calcite, $CaCO_3$ (Maslen, Streltsov & Streltsova, 1993), is far from that often considered as typifying covalent interactions, but this contradicts the Effenberger, Kirfel & Will (1983) interpretation of positive $\Delta\rho$ regions at the mid-points of the Ca—O and Mg—O vectors in dolomite, $CaMg(CO_3)_2$, in terms of covalency in those bonds.

Göttlicher & Vegas (1988) observation of an electron-density bridge between O atoms along the longest edge of the MgO_6 octahedron contrasts with lower density near a short O—O distance outside that octahedron, which in magnesite is among the shortest non-bonding O—O contacts for all calcite-type carbonates (Effenberger, Mereiter & Zemann, 1981). No similar $\Delta\rho$ increase along the longest edge of the CaO_6 octahedron occurs in calcite (Maslen, Streltsov & Streltsova, 1993). The density increased slightly between the short edge of the CaO_6 octahedron and near the mid-point of the short non-bonding contact between O atoms. Magnesite and calcite span the extreme range of lengths for this contact in the isomorphous carbonate minerals.

In most electron-density studies carried out so far, extinction was corrected by least-squares fitting of extinction parameters for structure factors from a crystal model to the observed structure factors. Those extinction parameters correlate strongly with the scale factor and some model parameters. Least-squares minimization of a residual may be so ill-conditioned that small adjustments to the weight of the observations alter the extinction correction drastically, introducing artefacts (Streltsov & Maslen, 1992).

Correlation of extinction parameters with the scale-factor and model parameters can be avoided. The extinction corrections for large magnesite slabs cut parallel to a desired face in the study by Gött-

licher & Vegas (1988) do not rely on theoretical structure factors. Unfortunately, that study was based on expressions (1) and (2) for extinction (Zachariasen, 1967), which omit a sin 2θ dependence for $t_\perp$ (Becker & Coppens, 1974).

A method applicable to small crystals that does not require model structure factors (Maslen & Spadaccini, 1993), used to evaluate extinction corrections for calcite (Maslen, Streltsov & Streltsova, 1993), is applied below to magnesite. This provides an opportunity to compare $\Delta\rho$ maps obtained by two extinction correction methods, both independent of theoretical structural models, noting the limited reproducibility of X-ray diffraction $\Delta\rho$ maps reported by Dam *et al.* (1984) for oxalic acid dihydrate.

Experimental

A cleavage fragment of magnesite from the Mineralogical Museum of the University of Western Australia selected for the X-ray diffraction measurements was bounded by two $\{\bar{1}14\}$, two $\{104\}$ and two $\{0\bar{1}4\}$ faces $24 \times 57 \times 81$ μm, respectively, from the crystal centre. The dimensions were measured and faces indexed using optical and Philips SEM505 scanning electron microscopes. The sample was analysed by extended X-ray absorption fine-structure spectroscopy (EXAFS). Ca and Fe impurities were negligible.

Diffraction data were measured on a Syntex $P3$ four-circle diffractometer with Mo $K\alpha$ radiation ($\lambda = 0.71073$ Å) monochromated with an oriented graphite monochromator in the equatorial setting. Lattice constants were determined from 24 reflections with 2θ values $30.4 < 2\theta < 47.38°$. Reflection intensities were for a complete sphere with $(\sin\theta/\lambda)_{max} = 1.079$ Å^{-1}, $-10 \le h \le 10$, $-10 \le k \le 10$, $-32 \le l \le 32$ using $\theta/2\theta$ scans. Six standards were monitored every 100 reflections. Integrated intensities were evaluated using a profile-analysis program (Streltsov & Zavodnik, 1989). Variances in measured structure factors from counting statistics were modified for source instability indicated by the standards as suggested by Rees (1977) and then by comparing equivalent reflection intensities following a Fisher test. Reflection variances consistent with Poisson statistics were not altered. Those for other reflections were adjusted to reflect the scatter of equivalents.

The linear absorption coefficient μ at Mo $K\alpha$ was evaluated from atomic absorption coefficients by Creagh (1992). Lorentz and polarization corrections were applied and absorption corrections (Alcock, 1974) evaluated analytically. Thermal diffuse-scattering corrections, estimated with the program *TDS2* (Stevens, 1974) using elastic constants for magnesite by Humbert & Plique (1972) were negligible. Extinction corrections for the full data sets were determined by optimizing the isotropic extinction coefficient r^* in the correction formula of Larson (1970) by least-squares minimization of differences between intensities for equivalent reflections with different path lengths (Maslen & Spadaccini, 1993) before structural parameters were refined. All calculations utilized the *Xtal*3.2 crystallographic programs (Hall, Flack & Stewart, 1992) implemented on DEC 5000/120 workstations.

Table 1. *Experimental and refinement data for* $MgCO_3$

Radiation	Mo $K\alpha$
λ (Å)	0.71073
Diffractometer	Syntex $P3$
Monochromator	Graphite
Scan speed (° min^{-1})	3.08
Peak scan width $[l + r + (2\theta_{K\alpha1} - 2\theta_{K\alpha2})d]$	0.9; 1.0; 1.0
Max. 2θ (°)	100
Max. intensity variation of standards $[\pm(\bar{4}44), \pm(0\bar{1}4), \pm(202)]$ (%)	4.1
No. of measured reflections	3508
Transmission range	0.914; 0.979
No. of independent reflections	332
Extinction,† r^*	0.64 (2) × 10^3
Min. extinction,‡ y (hkl)	0.93, $(\bar{1}14)$
$R_{int}(F^2)$, before	0.025
after absorption	0.022
extinction applied	0.021
R	0.022
wR	0.025
S	5.87
Max. shift/e.s.d.	0.0001

† Maslen & Spadaccini (1993) approach.
‡ $F_o = yF_{kin}$, where F_{kin} is the value of the kinematic structure factor.

The reference-state structure-factor calculations were for the independent atom model (IAM), evaluated with spherical atomic scattering factors from *International Tables for X-ray Crystallography* (1974, Vol. IV), and dispersion corrections $\Delta f'$, $\Delta f''$ of 0.049, 0.037 for Mg, 0.007, 0.002 for C, and 0.018 0.006 for O at Mo $K\alpha$ by Creagh (1992). Ten independent parameters, including anisotropic vibration tensor elements, were determined by full-matrix least-squares refinement based on $|F|$ with least-squares weights equal to $1/\sigma^2(F_o)$ for all measured structure factors. Further details are given in Tables 1 and 2.† Extinction corrections corresponding to the significantly negative r^* parameter (Larson, 1970) evaluated during structure refinement were not applied. The small positive r^* value obtained by the Maslen & Spadaccini (1993) approach was preferred. Local small positive $\Delta\rho$ peaks at the nuclear sites could be attributed to statistical uncertainties in the least-squares scale factor.

† Lists of structure factors have been deposited with the British Library Document Supply Centre as Supplementary Publication No. SUP 71270 (5 pp.). Copies may be obtained through The Technical Editor, International Union of Crystallography, 5 Abbey Square, Chester CH1 2HU, England. [CIF reference: AS0629]

Table 2. *Fractional coordinates x, anisotropic vibration parameters U_{ij} (Å^2), rigid-body parameters and selected interatomic distances* (Å) for $MgCO_3$

6 Mg on 6(*b*)	U_{11}	0.0058 (1)	T_{11} (Å^2)	0.004 (2)
(0,0,0)	U_{33}	0.0067 (2)	T_{33} (Å^2)	0.0076 (6)
			L_{11} (rad^2)	0.0003 (6)
6 C on 6(*a*)	U_{11}	0.0059 (3)	L_{33} (rad^2)	0.00016 (6)
(0,0,¼)	U_{33}	0.0054 (4)	S_{11} (rad^2)	0.0003 (3)
18 O on 18(*e*)	x	0.2774 (1)	C—O	1.2857 (3)
(x, 0, ¼)	U_{11}	0.0056 (1)	C—O	[1.2870 (3)]*
	U_{22}	0.0079 (2)	Mg—O^i	2.1029 (3)
	U_{33}	0.0092 (2)	O—O1^{ii}	2.2269 (5)
	U_{13}	−0.00054 (8)	O—O2^i	2.8502 (3)
			O—O3^{iii}	2.9265 (7)
			O—O4^{iv}	3.0206 (4)

Symmetry code: (i) $\frac{2}{3} - x, \frac{1}{3} - y, \frac{1}{3} - z$; (ii) $-y, x - y, z$; (iii) $1 - y, x - y, z$; (iv) $\frac{2}{3} + y, \frac{1}{3} - x + y, \frac{1}{3} - z$.

* The C—O distance corrected for riding motion.

Least-squares methods may be biased significantly if large differences between the observed data and model predictions occur more frequently than expected for a normal distribution. Least-squares residuals for the magnesite structure refinement were dominated by four low-angle reflections with $|F_o - F_c|/\sigma$ values greater than 30, including a value of 57 for the 006 reflection. For three of these reflections $|F_o|$ exceeds $|F_c|$ predicted by the model. In decreasing those residuals the least-squares process generated a significant negative extinction parameter and biased the scale factor. This was confirmed by reducing the weights for those reflections to satisfy the Gauss–Markov conditions (*e.g.* Prince, 1982) for validity in least-squares processes. This eliminated the $\Delta\rho$ peaks at the nuclei without changing density features elsewhere appreciably. A scale factor refinement assigning unit weights to every reflection after the structural parameters were determined gave similar results. Note that the $\Delta\rho$ maps for magnesite presented by Göttlicher & Vegas (1988) are based on unit-weighted structure refinement.

Structural parameters

The Mg cation with six coordinating O atoms forms an octahedron (Fig. 1) slightly flattened in the direction of the hexagonal *c* axis, as in calcite (Maslen, Streltsov & Streltsova, 1993). The O—O3 lengths parallel to the basal plane are less than those inclined to the base O—O4 (Table 2). The length of the O—O edge of the regular coordination octahedron is intermediate throughout the cubic oxides (Lippmann, 1973). The octahedron distortion ratio (longer/shorter edge) of 1.0321 (3) in magnesite, being small compared to 1.0459 (6) in calcite, may indicate that the small Mg cation coordinates more ideally with the O anions, but such ratios are not monotonic functions of the *M*—O distance, and cannot be explained by electrostatic interactions alone (Effenberger, Mereiter & Zemann, 1981). The octahedral distortions in the rhombohedral carbonates may reflect particular characteristics of the electron density in the CO_3 group.

The cation–oxygen distances in the rhombohedral carbonates are smaller than those in the cubic oxides and are also smaller than the sums of the Göldschmidt ionic radii (Lippmann, 1973), except for magnesite. All interatomic distances in Table 2 are close to recently refined values for calcite-type carbonates (Effenberger, Mereiter & Zemann, 1981). The C—O bond length in magnesite is within 2 e.s.d.'s of that for calcite reported by Maslen, Streltsov & Streltsova (1993).

The vibration ellipsoid for Mg in magnesite is elongated along *c* (Table 2), whereas the Ca ellipsoid in calcite (Maslen, Streltsov & Streltsova, 1993) is an oblate spheriod. The CO_3 group in calcite-type structures has site symmetry 32. Its rigid-body motions may be represented by five independent coefficients, two each for T and L and one for S (Schomaker & Trueblood, 1968). Values compiled in Table 2 are within 1 e.s.d. (2 e.s.d.'s for L_{11}) of coefficients refined by Finger (1975).

Electron density

Atomic charges determined by projecting $\Delta\rho$ onto atomic density basis functions (Hirshfeld, 1977) are for Mg +0.05 (3), C +0.16 (2) and O −0.07 (1) e. The ordering of these charges as in calcite (Maslen, Streltsov & Streltsova, 1993) reflects atomic electronegativities, and the C-atom charge is within 3 e.s.d.'s of the calcite value, but the Mg and O charges are significantly less than corresponding calcite values.

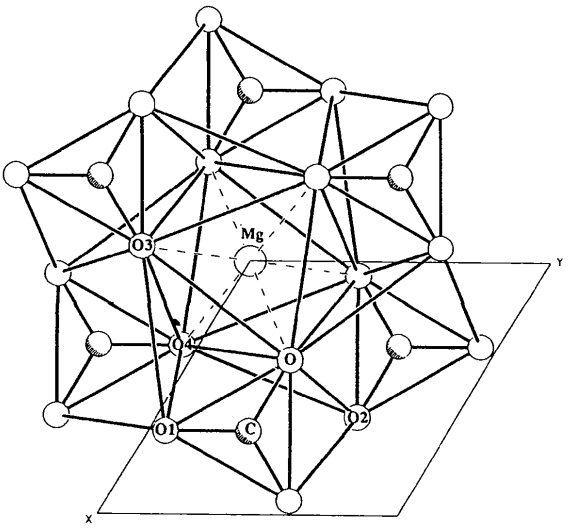

Fig. 1. Projection down the hexagonal *c* axis of a portion of the structure showing the central Mg coordinated to six O atoms from the distinct CO_3 groups.

Sections of magnesite $\Delta\rho$ in the (0001) plane through C and O, in the (01$\bar{1}$0) plane through Mg, C and O, and in the equatorial plane of the Mg octahedron shown in Fig. 2 are based on extinction corrections by the method of Maslen & Spadaccini (1993). The 0.1 e Å^{-3} contour interval is more than three times $\sigma(\Delta\rho) = 0.03$ e Å^{-3} evaluated by the Cruickshank (1949) method. In showing no evidence of CO_3 group disorder or deviation from planarity, the Fig. 2(*a*) and 2(*b*) $\Delta\rho$ maps are consistent with those for calcite. Most $\Delta\rho$ maxima for magnesite are higher than those for calcite. This can be attributed to increased exchange depletion when the more diffuse Ca valence-electron distribution overlaps with the CO_3 group.

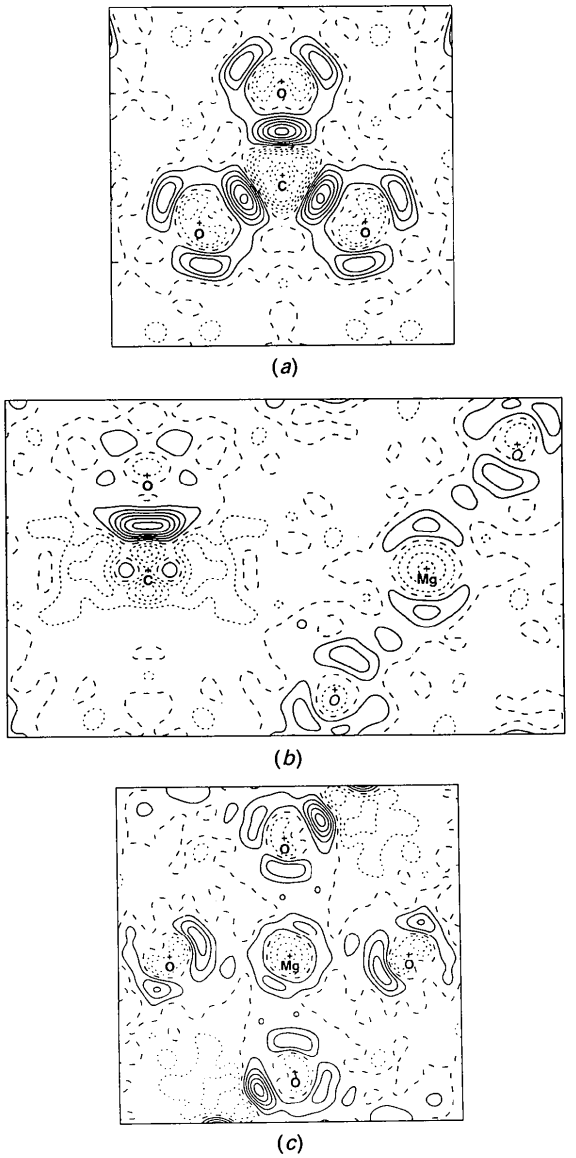

Fig. 2. $\Delta\rho$ for $MgCO_3$, evaluated with extinction corrections that minimize differences between equivalent reflection intensities. (*a*) (0001) plane through three O atoms of the CO_3 group; map borders 4.6 by 4.6 Å. (*b*) (01$\bar{1}$0) plane through Mg, C and O atoms with two O atoms deviating from the plane by 0.22 Å shown in italics; map borders 7.5 by 4.6 Å. (*c*) Equatorial plane of an MgO_6 octahedron; map borders 6 by 6 Å. Contour interval 0.1 e Å $^{-3}$, positive, negative contours – solid, short dashes, respectively.

Positive $\Delta\rho$ peaks 0.66 e Å^{-3} high at the middle of each C—O bond and 0.35 e Å^{-3} peaks in O lone-pair regions in Fig. 2(*a*) are within 3 e.s.d.'s of those reported by Göttlicher & Vegas (1988). Two O lone-pair peaks subtend an angle of about 125° at the nucleus. The Fig. 2(*b*) lone-pair maxima above and below O, polarized towards Mg, subtend an angle of about 80° at the O nucleus. Elongation of C—O maxima perpendicular to the bond line in the basal plane (Fig. 2*a*) and in the *c* direction perpendicular to the C—O bond (Fig. 2*b*) may indicate π bonding between the C and O atoms.

The weak maximum near the middle of the Mg—O bond depicted in Figs. 2(*b*) and 2(*c*), less than 0.1 e Å^{-3} high, suggests minimal $\Delta\rho$ σ-type covalent character in the Mg—O bonding. On the other hand extension of the density maximum on the C—O bond, parallel to the Mg—O vector in Fig. 2(*b*), and a similar weaker feature near Mg would be consistent with some π character in the Mg—CO_3 interaction.

There is no increase in density along the longest edge of the MgO_6 octahedron, of length 3.0206 (4) Å, in Fig. 2(*c*), resembling that reported by Göttlicher & Vegas (1988). $\Delta\rho$ is depleted there as well as at the mid-point of the short non-bonding contact between the O atoms (map not presented), of length 2.8502 (3) Å, which is not an edge of the MgO_6 octahedron.

Concluding remarks

As calcite and magnesite grow from solution, lattice defects are introduced into their structure (Wenk, Barder & Reeder, 1983), forming crystals of low perfection. This electron-density study on magnesite, with that on calcite by Maslen, Streltsov & Streltsova (1993), successfully applies extinction corrections from equivalent reflections (Maslen & Spadaccini, 1993), which do not rely on theoretical structural models. This approach, based on Zachariasen (1967) theory, is applicable to small crystals. For microcrystals with dimensions less than 1 μm, kinematic conditions of diffraction are necessarily fulfilled. Diffraction from larger crystals approaches this limit asymptotically as their size is reduced, at a rate dependent on the size and distribution function for the perfect microdomains of which the real crystal is composed. The use of sufficiently small crystals reduces the effects of secondary extinction, and thus

improves the accuracy of strong low-order structure factors which are important for deformation electron-density studies. To provide high-precision measurements of the weaker structure factors an intense X-ray source, such as synchrotron radiation, is then desirable.

We acknowledge Dr Dudley Creagh here for his calculations of absorption coefficients and dispersion corrections. This work was supported by the Australian Research Council.

References

ALCOCK, N. W. (1974). *Acta Cryst.* A**30**, 332–335.
BECKER, P. J. & COPPENS, P. (1974). *Acta Cryst.* A**30**, 129–147.
CREAGH, D. C. (1992). Personal communication.
CRUICKSHANK, D. W. J. (1949). *Acta Cryst.* **2**, 65–82.
DAM, J., HARKEMA, S., FEIL, D., FELD, R., LEHMAN, M. S., GODDARD, R., KRUGER, C., HELLNER, E., JOHANSEN, H., LARSEN, F. K., KOETZLE, T. F., MCMULLAN, R. K., MASLEN, E. N., STEVENS, E. D. & COPPENS, P. (1984). *Acta Cryst.* A**40**, 184–195.
EFFENBERGER, H., KIRFEL, A. & WILL, G. (1983). *Tschermaks Mineral. Petrogr. Mitt.* **31**, 151–164.
EFFENBERGER, H., MEREITER, K. & ZEMANN, J. (1981). *Z. Kristallogr.* **156**, 233–243.
FINGER, L. W. (1975). *Carnegie Inst. Washington Yearb.* **74**, 572–575.
GÖTTLICHER, S. & VEGAS, A. (1988). *Acta Cryst.* B**44**, 362–367.
HALL, S. R., FLACK, H. D. & STEWART, J. M. (1992). Editors. *Xtal3.2 Reference Manual.* Univs. of Western Australia, Australia, and Maryland, USA.
HIRSHFELD, F. L. (1977). *Isr. J. Chem.* **16**, 198–201.
HUMBERT, P. & PLIQUE, F. (1972). *C. R. Acad. Sci. Ser. B*, **275**, 391–394.
LARSON, A. C. (1970). In *Crystallographic Computing*, edited by F. R. AHMED. Copenhagen: Munksgaard.
LIPPMANN, F. (1973). *Sedimentary Carbonate Minerals.* Berlin: Springer-Verlag.
MASLEN, E. N. & SPADACCINI, N. (1993). *Acta Cryst.* A**49**, 661–667.
MASLEN, E. N., STRELTSOV, V. A. & STRELTSOVA, N. R. (1993). *Acta Cryst.* B**49**, 636–641.
PRINCE, E. (1982). *Mathematical Techniques in Crystallography and Materials Science.* New York: Springer-Verlag.
REES, B. (1977). *Isr. J. Chem.* **16**, 180–186.
SCHOMAKER, V. & TRUEBLOOD, K. N. (1968). *Acta Cryst.* B**24**, 63–76.
STEVENS, E. D. (1974). *Acta Cryst.* A**30**, 184–189.
STRELTSOV, V. A. & MASLEN, E. N. (1992). *Acta Cryst.* A**48**, 651–653.
STRELTSOV, V. A. & ZAVODNIK, V. E. (1989). *Sov. Phys. Crystallogr.* **34**(6), 824–828.
WENK, H.-R., BARDER, D. J. & REEDER, R. J. (1983). *Carbonates: Mineralogy and Chemistry. Reviews in Mineralogy*, Vol. 11, edited by R. J. REEDER, pp. 301–367. Chelsea, Michigan: Book Crafts.
ZACHARIASEN, W. H. (1967). *Acta Cryst.* A**23**, 558–564.

Acta Cryst. (1993). B**49**, 984–987

Single-Crystal Pulsed Neutron Diffraction from NiF_2 and FeF_2: the Effect of Magnetic Order on the Fluorine Positions

BY W. JAUCH AND A. PALMER

Hahn-Meitner-Institut, Glienicker Strasse 100, *D*-14109 *Berlin, Germany*

AND A. J. SCHULTZ

Chemistry and Materials Science Divisions, Argonne National Laboratory, Argonne, Illinois 60439, *USA*

(*Received* 9 *March* 1993; *accepted* 9 *July* 1993)

Abstract

Extended single-crystal data sets have been collected by means of pulsed neutron diffraction from NiF_2 at 295, 80 and 15 K, and from FeF_2 at 295 and 15 K to examine the effect of magnetic order on the fluorine nuclear positions. A predicted internal displacement has been validated in NiF_2, whereas in FeF_2 it could not be established unambiguously. The positional parameters are compared with those obtained from γ-ray diffraction data, recorded from the same samples. In view of the excellent agreement there is no evidence for any polarization effects in the antiferromagnetic phase.

1. Introduction

It has been predicted that the magnetic ordering in transition-metal difluorides is accompanied by small internal magnetostrictive shifts of the anions (Jauch, 1991). In MnF_2 such a shift has been established by extended γ-ray and neutron diffraction studies. In the magnetically ordered phase, however, the two methods did not yield identical results for the fluorine positional parameter (Jauch, McIntyre & Schultz, 1990). The significant difference can be attributed to a polarization of the fluorine core electron density (Jauch & Stewart, 1991). In the absence of neutron diffraction data this impact of magnetic